People's Democratic Republic of Algeria
Ministry of Higher Education and Scientific Research

Amar Telidji University of Laghouat

FACULTY: TECHNOLOGY

DEPARTEMENT: PROCESS ENGINEERING

MASTER THESIS

Submitted by: Hazel Mohamed Taha

Bentaireche Abdelhamid

DOMAINE: Sciences And Technology

SECTOR: Process Engineering

OPTION: Material Process Engineering

THEME

Theoretical investigation of structural electronic, and optical properties of the cubic cesium iodate C-$CsIO_3$

Jury members:

First and last name	Grade	Quality
BOUTASSOUNA Nassima	MCB	President
BOUREZG Mohamed Tahar	MCB	Examiner
BELHADJ Soraya	MCB	Advisor

Promotion: 2025 - 2026

Dedication

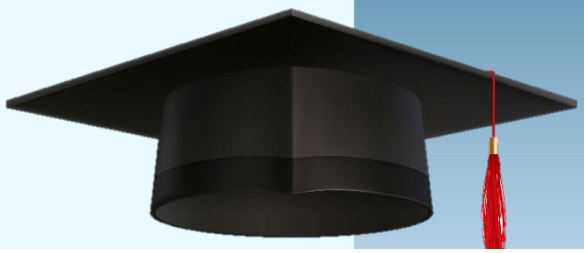
I dedicate this work to my beloved parents.
To my brothers and sisters and our supervisor.
I want to express my deep gratitude and thanks to all those who have supported me throughout my academic career.
You have all my gratitude and appreciation.

HAZEL Mohamed Taha

Dedication

To my family, my friends, our supervisor, and all those who believed in me,
Thank you for your encouragement, your presence, and your comforting words in moments of doubt.
This thesis is also somewhat yours.

BENTIRECHE Abdelhamid



Acknowledgments

First of all, we thank ALLAH, the Almighty, who gave us strength, health and courage to complete our project.

We express our most sincere gratitude to our parents. It is thanks to their love, patience, sacrifices and constant support, both moral and material, that we have been able to build this journey. Without their presence, none of this could have happened.

We would like to thank our supervisor, Dr. BELHADJ Soraya, for his availability, valuable advice and constant support throughout this project. His insight and scientific rigor have considerably nourished our reflection.

Also, we gratefully thank Dr. BOUTASSOUNA Nasssima and Dr. BOUREZG Mohamed Tahar to the honor of examining the present work.

We wish to express our sincere gratitude to all those who, directly or indirectly, participated in the preparation of this manuscript.

We would also like to express our gratitude to all the teachers for the excellence of the work and the professional environment provided throughout our training.

List of Abbreviations

Abbreviation	Full meaning
BC	Conduction Band
BFGS	Broyden-Fletcher-Goldfarb-Shanno
BV	Valence Band
BZ	Brillouin Zone
CB	Conduction Band
CIF	Crystallographic Information File
DFPT	Density Functional Perturbation Theory
DFT	Density Functional Theory
DOS	Density of States
Eg	Energy Gap
FP-LAPW	Full Potential Linearized Augmented Plane Wave
GGA	Generalized Gradient Approximation
IBZ	Irreducible Brillouin Zone
NCS	Non-Centrosymmetric
NLO	Nonlinear Optics
PDOS	Partial Density of States
RMT	Muffin-Tin Radius
SHG	Second Harmonic Generation
TB-mBJ	Tran-Blaha modified Becke-Johnson
VB	Valence Band
VESTA	Visualization for Electronic and Structural Analysis
WC-GGA	Wu-Cohen Generalized Gradient Approximation

List of Figures

Figure N°	Title	Page
Figure II.1	Cubic primitive cell of C-$CsIO_3$	13
Figure II.2	Structural parameter optimization: Volume optimization for C-$CsIO_3$	13
Figure II.3	Calculated band structure for C-$CsIO_3$ with TB-mBJ	15
Figure II.4	Total and partial density of states calculated for C-$CsIO_3$ with TB-mBJ	15
Figure II.5	Charge density calculated for C-$CsIO_3$	16
Figure II.6	Calculated imaginary $\varepsilon_2(\omega)$ and real $\varepsilon_1(\omega)$ parts of the dielectric function for C-CsIO3 with TB-mBJ	17
Figure II.7	Calculated optical properties for C-CsIO3 as function of the incident photon energy (eV): absorption coefficient I, reflectivity R, energy loss L, and refraction index n	19

List of Tables

Table No.	Title	Page
Table II.1	Valence state and Muffin-Tin rays RMt of C-$CsIO_3$ constituent elements	12
Table II.2	The k-points grid (points of sampling of Irreducible Brillouin Zone IBZ)	12
Table II.3	C-$CsIO_3$ structural parameters	13
Table II.4	Atomic coordinates for C-$CsIO_3$ (all are general positions)	13
Table II.5	Simulated and experimental structural parameters of C-$CsIO_3$	14
Table II.6	Results related to band structure calculation of C-$CsIO_3$	15
Table II.7	Static refractive index calculated for C-$CsIO_3$	18
Table II.8	Energy loss L(ω) for C-$CsIO_3$	19
Table II.9	Optical gap values (energy at I0) for C-$CsIO_3$	19
Table II.10	Values of the birefringence (Δn) for the compound C-$CsIO_3$	19

List of content

Table of content

General introduction 01

References 02

Chapter I: Bibliographic review

I.1. Introduction 03

I.2. Strategies for designing non-centrosymmetric structures 03

I.2.1. Acentricity problem 03

I.2.2. Principle of nonbonded electron pairs (lone pairs) 03

I.2.3. "Additive" effect of distortions 04

I.3. Iodates: a family of promising NLO materials 05

I.3.1. Anionic group IO_3^- 05

I.3.2. Survey of important iodate NLO crystals 06

I.3.2.1 Alkali metal iodates (MIO_3) 06

I.3.2.2. Transition metal iodates 06

I.4. First-principles computational methods 06

I.4.1. Introduction to density functional theory (DFT) 06

I.4.2. Calculating optical properties 07

I.4.2.1. Linear optical properties 07

I.4.2.2. Band gap correction (scissor operator) 07

I.4.2.2. Nonlinear optical properties (SHG) 08

I.4.4. Techniques for analysis: spectral and spatial decomposition 08

References 10

Chapter II: Results and discussion

II.1. Introduction 11

II.2. Calculation details and parameters 11

II.2.1. Methods adopted 11

II.2.2. Code Wien2k 11

II.2.3. Convergence step 11

II.2.4. Optimization step 12

II.3. Study of the compound C-$CsIO_3$ 12

II.3.1. Structural properties of C-$CsIO_3$ 13

II.4. Calculated structural properties of C-$CsIO_3$ 13

II.5. Calculated electronic properties 14
II.5.1. Band structure 14
II.5.2. Density of states 15
II.5.3. Charge densities 16
II.5.4. Charge densities 16
II.5.4.1. Dielectric function 16
II.5.4.2. Static refraction indices 18
II.5.4.3. Other linear optical properties 18
II.6. Conclusion 19
References 21
General conclusion 22

General introduction

Currently, an extremely rapid development in the field of creation of functional inorganic materials has occurred. This type of materials finds wide application in technology, in particular, lasers, optical communications, photovoltaics, and optoelectronics. The alkali metal iodates occupy an important position among the aforementioned materials because of their specific structure, which ensures a great potential for applications related to nonlinear optics [1,2].

Thus, cesium iodate $CsIO_3$ deserves special consideration. This compound exhibits excellent optical properties related to its non-centrosymmetric crystal structure and includes, for example, strong second-harmonic generation, high transparency in wide spectral regions, and high damage threshold under laser irradiation [3]. Due to these properties, $CsIO_3$ can be considered as a material with the highest potential among alkali metal iodates [2,4].

Nevertheless, the knowledge of basic electronic and structural properties is also very important for the creation of new materials, and, at that, it can be obtained through first-principles calculations performed using density functional theory [1,4]. First-principles methods allow obtaining information about the electronic structure and properties of a material without performing any experimental work, which may require the synthesis of materials [5].

The main purpose of the work presented in this thesis is to perform an extensive theoretical study on the cubic $CsIO_3$ phase that will shed light on the electronic and optical properties of the structure. Through the analysis of structural characteristics, electronic density of states, and linear optical responses such as the dielectric function and refractive index of the structure, a complete and precise description can be obtained about the physical properties of the cubic structure under study. In addition, another important objective is to assess the mechanical stability and the possible uses of the cubic high-symmetry structure.

Our work is organized into the following parts:

- General introduction.
- Chapter I: Bibliographic review.
- Chapter II: Calculations, results and discussion.
- General conclusion.

References

[1] P.S.H. and K.R. Poeppelmeier. Noncentrosymmetric oxides. Chemistry of Materials, vol. 10, N°110, pp. 2753-2769, 1998.

[2] C.L.H. and J.G. Mao. Recent advances on second-order NLO materials based on metal iodates. Coordination Chemistry Reviews, vol. 288, pp. 1-17, 2015.

[3] C.H.T.A.Z.Y. and S.P.M. Zhang. Functional materials design via structural regulation originated from ions introduction: A study case in cesium iodate system. Chemistry of Materials, vol. 30, N°14, p. 1136–1145, 2018.

[4] K.M. Ok. Toward the rational design of novel noncentrosymmetric materials: Factors influencing the framework structures. Accounts of Chemical Research, vol. 49, N°112, pp. 2774-2785, 2016.

[5] K.B. and M.E.J.P. Perdew. Generalized gradient approximation made simple. Physical Review Letters, vol. 77, N°118, pp. 3865-3868, 1996.

Chapter I:

Bibliographic search

I.1. Introduction

Nonlinear optical materials play a crucial role in the development of photonics. These materials have the potential to interact with light and matter to produce new frequencies [1]. The development of nonlinear optical materials has revolutionized laser devices, communication systems, medical diagnostics, and defense systems.

I.2. Strategies for designing non-centrosymmetric structures

I.2.1. Acentricity problem

The ability to develop second-order nonlinear optical (NLO) materials is directly dependent on the ability to create noncentrosymmetric (NCS) structures, as second-order susceptibility ($\chi^{(2)}$) is zero in centrosymmetric structures [1]. However, it has been a significant problem in understanding and predicting which materials will possess noncentrosymmetric structures. Bergman et al. emphasized this point, commenting that "One of the major unresolved questions which has not previously been dealt with is how to predict in advance which materials will have acentric structures. This is particularly crucial since the incidence of acentric structures is low (∼20%) in inorganic materials" [2]. The fact that only 20% of inorganic compounds have noncentrosymmetric structures indicates that it is imperative to develop strategies that will assist in the search for NLO materials.

I.2.2. Principle of nonbonded electron pairs (lone pairs)

One important discovery for the development of this concept was introduced by Bergman et al., who developed a general rule about the stereochemical activity of nonbonded electrons [2]. According to their research, the molecules or ions BO_2^{-n} are lacking a point of symmetry when the element B has nonbonded electrons. "The challenge of obtaining an acentric crystal is met by using acentric oxygen polyhedra as structural units." [2] One example of a molecule that fits into this concept is the iodates. In the compound IO_3^-, the I^{5+} ion has an active stereochemical lone pair of electrons, which makes it distort the coordination geometry and results in an asymmetric trigonal pyramid [2]. Bergman et al. found that this approach is characterized by a very high percentage of acentricity: "In this paper, we present a general principle that involves nonbonded electrons and demonstrate that it yields classes of materials with an acentricity frequency approaching 100%." [2].

This thesis was supported experimentally via SHG and piezoelectric studies of different iodates: "With the exception of $NaIO_3$, all the materials give positive piezoelectric responses... the results obtained from piezoelectric and SHG experiments, which indicate a high frequency of acentricity among molecules containing ions of the type BO_2^{-n}, with B having an unshared electron pair, clearly demonstrate the correctness of the thesis put forward at the beginning of this paper" [2]. This distortion may be estimated through bond-length difference in the IO_3^- ion. In particular, Bergman et al. presented data on bond length distortions in different iodates in their Table I. For instance, the distortion of the ion of HIO_3 is $\Delta = 0.85$ Å, whereas that for $LiIO_3$ equals $\Delta = 1.05$ Å [2].

I.2.3. "Additive" effect of distortions

Another design concept that can further improve the NLO performance is the use of a combination of polar components, which would result in a better total performance through the additive effect of polarization. Hu and Mao discussed this design concept in detail: "Of these concepts, the combination of d^0 transition metal ions (Ti^{4+}, V^{5+}, Nb^{5+}, Mo^{6+}, W^{6+}, etc) and stereo electronic lone pairs of cations (Se(IV), Te(IV), I(V), etc), both of which undergo SOJT distortion, has been found to be very successful in designing polar compounds with good second-order NLO properties owing to their 'additive' polarization effects" [1].

The strategy has been successful in the case of $AMoO_3(IO_3)$ compounds that have a combination of MoO_6 distorted octahedra (from the d^0 Mo^{6+} cation) along with distorted IO_3^- groups (the I^{5+} cation, which has one lone pair of electrons). Such compounds result in highly polarized structures characterized by huge local dipole moments. The Mo^{6+} cation is found to experience intra-octahedral distortion toward a face of the MoO_6 octahedron (C_3 distortion) with a local dipole moment of 9.20 D... The I^{5+} cations in these materials are in distorted trigonal pyramidal coordination, with the local dipole moments for the IO_3^- groups being 5.21, 5.89 and 5.73 D for the Li, Rb and Cs compounds, respectively" [1].

The macro-polarity of the crystal arises due to the geometrical orientation of these polar structural units. As Hu and Mao stated, "due to the symmetry requirement of the crystal structure, the polarization directions of the distorted units are reversed in some coordinate axes and the dipole moment gets canceled out… only the dipole moment along the b-axis for Li and along the c-axis for Rb and Cs compounds remain" [1]. Such comprehension

of how the macro-polarity can be created by these polar units is essential in developing the rational structure of the NCS.

Liu *et al.* (2018) provide another example of successful application of the concept in their study of the $A_2Ge(IO_3)_6$ system, in which the type of the cation at the A site plays a crucial role in determining the spatial distribution of the IO_3 units: "The variation of alkali metal ionic radius from Li^+ to K^+, Cs^+ has been found to affect significantly the coordination environment that changes the arrangement of polar [IO_3] anionic groups, resulting in a shift of the crystal structure from the NCS structure of $P6_3$ in $Li_2Ge(IO_3)_6$ to the CS structure of R3 in $A_2Ge(IO_3)_6$ (A = K, Rb and Cs)" [3].

I.3. Iodates: a family of promising NLO materials

1.3.1. Anionic group IO_3^-

IO_3^- anion constitutes the basic structural unit of iodate NLO compounds. The molecular geometry of this ion is a distorted trigonal pyramid with a central I^{5+} ion having a stereochemically active $5s^2$ lone pair [2].

The electronic theory of this distortion was explained by Bergman *et al.*: "Considering the simplest case of a BO_2^{-n} molecule like BO_3^{-n}, it is important to find out what should be done to distort the oxygen octahedron around the central B ion. If we consider the stereochemical activity of non-bonded electrons as a premise, then it can be concluded that the oxygen octahedron around the B ion is distorted when there is a non-bonded pair of electrons on the B ion."

The distortion of the iodates is considerable, as confirmed by the data on the bond length difference.

According to Bergman *et al.*, for $LiIO_3$: "$LiIO_3$: Short B-O = 1.82 Å, Long B-O = 2.87 Å, Δ = 1.05 Å" [2]. The high distortion value leads to the creation of a permanent dipole moment per every IO_3^- molecule, thus creating an appropriate polar building block in NCS crystal lattice.

Liu *et al.* also point out to the importance of the IO_3^- anion: "As known, iodates are a class of materials exhibiting a good transparency in the mid-IR atmospheric window of 3-5 μm. And [IO_3^-] anionic group as a polar building block with stereo chemically active lone-pair electrons on I^{5+} cation is very likely to give rise to NCS structure".

I.3.2. Survey of important iodate NLO crystals

I.3.2.1 Alkali metal iodates (MIO_3)

The alkali metal iodates represent the simplest class of iodate nonlinear optical (NLO) materials. These materials were studied by Bergman et al. in terms of powder SHG and piezoelectric properties: "The second member of the BO_3^{-n} series, MIO_3 (M = H, Li, Na, K, Rb, Cs, NH_4, and Tl were investigated for their acentricity by the use of SHG and piezoelectric effects. All but $NaIO_3$ produce positive piezoelectric response" [2].

The SHG values as the ratio R of SHG power to powdered quartz: HIO_3 (R=380), $LiIO_3$ (R=300), $NaIO_3$ (R=0), KIO_3 (R=2000), $RbIO_3$ (R=800), $CsIO_3$ (R=20), NH_4IO_3 (R=180), $TlIO_3$ (R=100) [2]. These data clearly indicate that most of the alkali metal iodates are acentric with significant SHG responses. The $CsIO_3$ (R=20), shows twenty times stronger SHG signal than quartz.

I.3.2.2. Transition metal iodates

The more complicated compounds contain iodate ions, such as IO_3^-, combined with the oxyanion ions of transition metals. The work by Hu and Mao on the $AMoO_3(IO_3)$ series (A = Li, Rb, Cs) stated: “According to the above theory, a large number of second-order nonlinear optical inorganic crystals have been synthesized. For example, the recently reported series of alkali metal-Mo(VI) iodates ($AMoO_3(IO_3)$ (A = Li, Rb, and Cs) are typical representatives that include the combination of distorted MoO_6 octahedral units and IO_3^- groups” [1].

I.4. First-principles computational methods

I.4.1. Introduction to density functional theory (DFT)

In the present era, DFT is recognized as an established technique to calculate and predict properties of NLO material by first principal calculation. Hu and Mao explained their method: "Calculations of electronic structure are carried out with a plane-wave basis set and pseudo-potentials using the density functional theory (DFT) in the total energy code CASTEP" [1]. The Perdew-Burke-Ernzehof functional (PBE) in the framework of the GGA approximation was used.

Liu et al. employed CASTEP program but considered the LDA method for the determination of exchange-correlation energy: "Total energy calculation based on density functional theory (DFT), plane wave/pseudopotential level, was performed by CASTEP

software, to seek out the minimum of electron energy and predict its optical properties, while the local density approximation (LDA) was selected to describe the exchange-correlation energy" [3].

The methods employed by Belhadj et al. were two different codes, namely WIEN2K and ABINIT. In WIEN2K, the method used was the FP-LAPW method with both GGA and TB-mBJ potentials. In ABINIT, the PP-PW method using LDA [4, p. 134] was used. It is important to note that the TB-mBJ potential gives a more accurate estimation for the band gap compared to the GGA method [4].

I.4.2. Calculating optical properties

I.4.2.1. Linear optical properties

The linear optical properties were derived from frequency dependence of the dielectric function. Liu et al. described, "From the scissor corrected electron structure, the optical absorption (the imaginary part of the dielectric function) can be obtained via electronic transition across the forbidden gap. Then using the Kronic-Kramer transformation, the refractive index (the real part) could be calculated" [3].

Belhadj et al. provided even more information. They obtained the imaginary part of the dielectric function using transition matrix elements between occupied and unoccupied states, and then using Kramers-Kronig transformation, they obtained the real part [4]. They pointed out that certain transitions contributed to particular peaks in the dielectric function: In the monoclinic phase, peaks around 5 eV result from O-p to I-p transition, while those at higher energies come from I-s and Cs-p state transitions [4].

I.4.2.2. Band gap correction (scissor operator)

One such issue related to DFT is its tendency to underestimate the band gaps. In this regard, Hu and Mao stated that "though the wave functions predicted by DFT-GGA are satisfactory, the CB energies cannot be predicted accurately. Therefore, the correction must be done using the 'scissor operator'" [1]. As a result, their obtained band gaps for $LiMoO_3(IO_3)$, $RbMoO_3(IO_3)$, and $CsMoO_3(IO_3)$ were 2.30, 2.23, and 2.34 eV respectively, which was considerably lower than the experimental results of 2.80, 3.10, and 3.10 eV respectively. This was because "it is well known that DFT-GGA is unable to provide accurate results for the eigenvalues of the electronic states" [1] .

Similarly, Liu et al. used the "scissor operator" for the same reason: "the band gap from LDA calculations will generally be smaller than that in the experiment because of the

discontinuity of the exchange-correlation energy, which is typical of the localized functional. Thus a 'scissor operator' has been applied to lift all the CB levels to the measured value" [3].

I.4.2.2. Nonlinear optical properties (SHG)

The calculation of the SHG coefficients needs to be done in a particular manner. Hu and Mao traced the history: "Numerical computation schemes for the second order optical susceptibility tensors of crystals have been intensively studied in the past few decades. In the early sixties, in 1963, Butcher and McLean introduced an approach for the calculation of the SHG coefficients from band structures, which unfortunately suffered from explicit divergences in their formulation. Subsequently, when Aspnes proposed a divergent-free formalism of cubic crystals, Ghahramani, Moss, and Sipe made another significant advancement by proposing a novel sum rule scheme" [1].

Hu and Mao adopted the scheme proposed by Duan and co-workers: "In recent years, Duan *et al.* investigated an evaluation scheme for reducing the k points required for convergence for the formula derived by Ghahramani et al. More specifically, the formula derived by Duan et al is straightforwardly linked to the electronic states, and the contribution from the electronic subsystem to the $\chi^{(2)}$ can be analyzed according to the spectral and spatial decomposition formulae suggested by them" [1].

Liu et al. relied on a different scheme that was developed independently within their group: "SHG coefficients were computed according to the formulas developed by our group using the model of virtual electron transition in length gauge approximation" [3].

Belhadj et al. computed the second-order optical susceptibilities using the PP-PW technique within LDA in the ABINIT package. The authors gave the values of the independent coefficients for the monoclinic (m symmetry) and rhombohedric (3m symmetry) phases, and the monoclinic phase had higher values than the other one [4].

I.4.4. Techniques for analysis: spectral and spatial decomposition

In order to determine the origin of SHG in these compounds, Hu and Mao used spectral and spatial decomposition: "To investigate the contribution from non-equivalent atoms or electronic states to the SHG response in these crystals, we perform the spectral and spatial decomposition according to previous studies" [1]. This technique allows the SHG coefficients to be divided by their contribution depending on energy and space.

Using the technique mentioned above, Hu and Mao managed to single out the major contributors to SHG in the studied $AMoO_3(IO_3)$ compounds: "The results show that the major contributions to $\chi^{(2)}$ in these compounds originate from the distorted MoO_6 and IO_3^- groups, i.e., the anionic group; while the contribution percentages of Rb^+ and Cs^+ cations (0.97 and 1.04, respectively) are far lower than that of Li^+ in $LiAMoO_3IO_3$ (5.71)" [1].

The results of the spectral decomposition allowed determining which electronic transitions were essential. According to the research conducted by Hu and Mao, "the SHG properties of these compounds can be mainly attributed to the interband electronic transition from the nonbonding O-2p states (i.e. the lone-pair electrons of O atoms) to the Mo-4d and some I-5p states" [1].

In their turn, Liu *et al.* carried out a similar investigation on the germanium iodates. They depicted the PDOS for all atom types and established that "the orbitals in iodine and oxygen dominate in the maximum of VB and minimum of CB, indicating that IO_3 groups account for the majority of SHG response in both two compounds, and the large deviation of the SHG effect in them mainly ascribe to the spatial arrangement difference of IO_3 group" [3].

To study bonding, Belhadj *et al.* examined the charge density map and found that "there are clear spherical symmetries of charge densities around Cs atoms with a very slight deviations towards O atoms, indicating the predominately ionic Cs-O bond character. Deformed contours around I and O atoms (both systems) explain the covalent character of I-O bonds" [4].

References

[1] C.-L. Hu et J.-G. Mao, «"First-principles study of electronic structures and nonlinear optical properties of $AMoO_3(IO_3)$ (A = Li, Rb and Cs) crystals",» *Journal of Physics: Condensed Matter,* vol. 22, n° %115, p. 155801, 2010.

[2] J. G. B. Jr., G. D. Boyd, A. Ashkin et S. K. Kurtz, «"New Nonlinear Optical Materials: Metal Oxides with Nonbonded Electrons",» *Journal of Applied Physics,* vol. 40, n° %17, pp. 2860-2863, 1969.

[3] X. J. X. W. L. Y. Z. L. Z. H. X. M. X. C. J. Q. H. Liu, «Influence of A-site cations on germanium iodates as mid-IR nonlinear optical materials: $A_2Ge(IO_3)_6$ (A = Li, K, Rb and Cs) and $BaGe(IO_3)_6H_2O$,» *Journal of Materials Chemistry C,* vol. 6, n° %117, pp. 4691-4700, 2018.

[4] B. L. M. B. T. a. D. B. S. Belhadj, «Structural, electronic, mechanical, linear and nonlinear optical, and piezoelectric properties of $CsIO_3$ materials from ab initio study,» *J. At. Mol. Condens. Matter Nano Phys,* vol. 8, n° %12, pp. 133-155, 2021.

Chapter II:

Results and discussion

II.1. Introduction

The materials considered in this study was investigated with regard to its structural, electronic, and optical properties via ab initio calculations using the calculation code Wien2k [1]. The materials studied is the cubic cesium iodate C-$CsIO_3$ [2].

II.2. Calculation details and parameters

II.2.1. Methods adopted

The calculation launch for each material with Wien2k is started by the manual introduction of an input density generated by the following data:

- Atomic number Z of each element in the material considered.
- Crystal system (Bravais lattice and space group).
- Cell parameters (a, b, c, α, β, and γ).
- Positions of atoms (x, y, z).

II.2.2. Code Wien2k

Calculations made with WIEN2k have the following details:

- Method: FP-LAPW; all electron (full potential-linearized augmented plane waves) [3].
- Approximation: WC-GGA (Wu and Cohn Generalized Gradient Approximation) [4].
- Exchange-correlation potential: TB-mBJ (Tran and Blaha modified Becke-Johnson potential) [5].
- Calculated properties: structural, electronic (band structure, total and partial density of states, and charge density) and linear optical (dielectric function ω, absorption coefficient I, reflectivity R, energy loss L, and refraction index n).
- Theory: DFPT (density functional perturbation theory) [6].

II.2.3. Convergence step

Before any calculation of properties, convergence studies followed by optimization must be carried out. In the convergence stage, the most important criteria are the relative variations of the total energy as a function of the calculation parameters: RK_{max} and ngkpt parameters.

It should be noted that the choice of the RMT rays (muffin-tin rays) of the atoms (table II.1) is made to reduce the interstitial space as much as possible, because this region is treated by plane waves, which makes the calculation time more important.

The values adopted for the calculation parameters are cross-referenced in (table II.2). For the $R_{MT}K_{max}$ parameter, it is taken equal to 7 (default values between 6 and 8).

Table II.1: Valence state and Muffin-Tin rays R_{MT} of C-$CsIO_3$ constituent elements.

Element	Valence state	R_{Mt}(Bohr)
Cs	$4d^{10}\ 5s^2\ 5p^6\ 6s^1$	2.0
I	$4d^{10}\ 5s^2\ 5p^5$	1.8
O	$2s^2\ 2p^4$	1.4

Table II.2: The k-points grid (points of sampling of Irreducible Brillouin Zone IBZ).

Compound	Grid(ngkpt)
C-$CsIO_3$	$10\times10\times10$[a]
	$16\times16\times16$[b]

[a] for the calculation of structural and electronic properties.
[b] for calculating optical properties.

II.2.4. Optimization step

The optimization step serves to relax the structure. An optimized structure corresponds to a minimum total energy, with atoms relaxed in a balanced environment translated by minimal resultant forces and Hellmann-Feynman forces (exerted on the atoms) canceled. The optimization is done using the BFGS program [7]. Often, several cycles are necessary to obtain a well-optimized structure.

It should be noted that optimization with Wien2k serves to relax the structure.

II.3. Study of the compound C-$CsIO_3$

We have invested the compounds C-$CsIO_3$ with regard to the calculation of its properties by the code Wien2k.

Our objective is to invest the above-mentioned properties by the introduction of the potential TB-mBJ (Tran and Blaha modified Becke-Johnson potential) in order to obtain more adequate values of the forbidden band (gap energies) [8]. The TB-mBJ potential turns out to be more precise in estimating the gap for materials containing metals in their structure.

In each step of the calculations (detailed below), our results were compared on one hand with experimental results, and on another hand with theoretical results (if existing).

II.3.1. Structural properties of C-$CsIO_3$

In figure II.1, the structure of our compound C-$CsIO_3$ is illustrated.

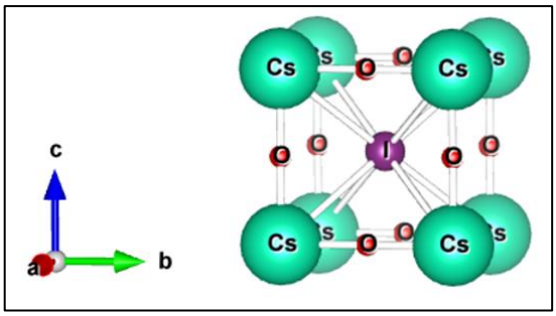


Figure II.1 Cubic primitive cell of C-$CsIO_3$.
Drawn from CIF file by VESTA software [9].

Table II.3: C-$CsIO_3$ structural parameters.

a (Å)	b (Å)	c (Å)	α/β/γ (°)	V(Å^3)/Z	Space group/N°	Crystal class	Ref.
4.662	4.662	4.662	90/90/90	101.33	Pm-3m/221	Cubic	[2]

Table II.4: Atomic coordinates for C-$CsIO_3$ (all are general positions) [2].

Atom	x	y	z
Cs	0	0	0
I	0.5	0.5	0.5
O	0	0	0.5

II.4. Calculated structural properties of C-$CsIO_3$

After the adoption of the calculation methods, the convergence steps, and the optimization of the structural parameters, the results are presented in figure II.2 (variation of volume vs. energy). Then, the optimized structural parameters are presented in table II.5

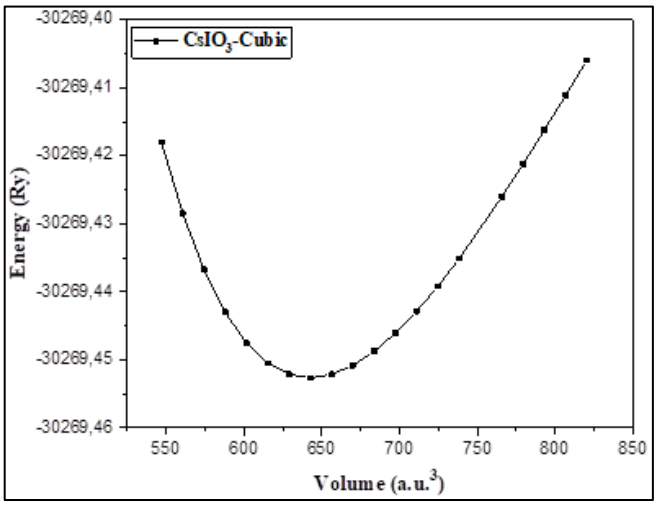


Figure II.2: Structural parameter optimization: Volume optimization for C-$CsIO_3$.

Table II.5: Simulated and experimental structural parameters of $CsIO_3$.

C-$CsIO_3$	Experimental [2]	This work (WC-GGA)	Deviation (%)
a=b=c (Å)	4.662	4.4601	-4.31
V(Å^3)	101.33	88.72	-12.44

From the results reported in table II.5, we note that the values of a, b, and c are estimated with acceptable deviations; 4.31% in absolute values. These results are consistent with the general trend of the GGA (FP-LAPW) approximation, which usually overestimates the structural parameters [10] (note here that the a and c-parameters have conversely been underestimated). Consequently, the volume is underestimated with tolerable discrepancy of 12.44%.

II.5. Calculated electronic properties

The electronic structures of C-$CsIO_3$ have been calculated and the following properties are reported:

- Band structure.
- Electronic densities.
- Density of states partial (PDOS) and total (DOS).

The main goal is to know the nature of the bonds between atoms.

II.5.1. Band structure

Figures II.5 and II.6 reflect the energies of the band structures calculated at the points of high symmetries in the Brouillon zone (BZ) by TB-mBJ.

There are two zones: the conduction band (BC) which corresponds to positive energies, and the valence band (BV) corresponding to negative energies. The latter consists of an inner layer (low energies far from the Fermi level) and an outer layer (near the Fermi level).

The following outcomes are to be illustrated:

- With TB-mBJ, we found out that our compound C-$CsIO_3$ undergoes a metallic behavior since he has no gap value (Eg=0eV) (figure II.5).
- Our iodate is considered as a good conductor; this means that it can be used for very different applications.

The obtained results are numerically reported in table II.6.

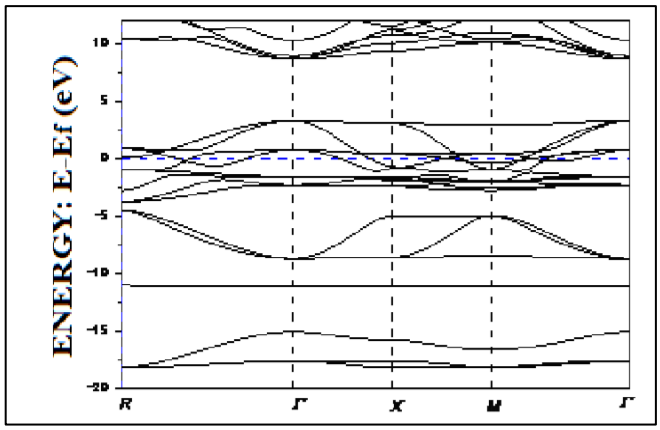


Figure II.3: Calculated band structure for C-$CsIO_3$ with TB-mBJ.

Tableau II.6: Results related to band structure calculation of C-$CsIO_3$.

Compound	WC-GGA	Energy gap (eV)			
		Nature	Value	Exp. [2]	Deviation (%)
C-$CsIO_3$	With TB-mBJ	Metallic	0	/	/
	Théorie	/	/		/

II.5.2. Density of states

Density of states is a very important physical property for solid phases. It determines the nature of bonding between atoms constituting the considered material.

Results related to the calculation of the density of states for our cubic iodate is illustrated in figure II.4.

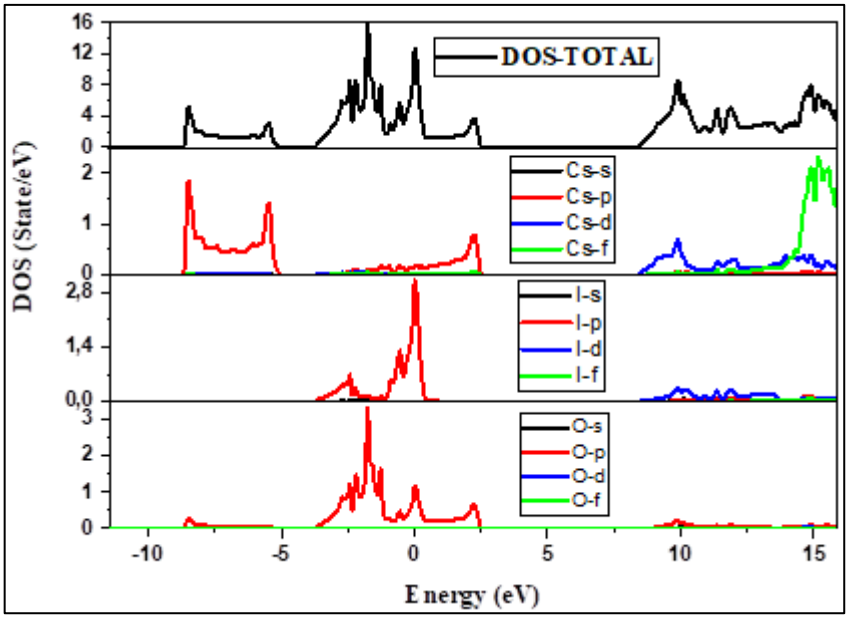


Figure II.4 Total and partial density of states calculated for C-$CsIO_3$.with TB-mBJ.

From this figure, we can clearly notice that states O-s, I-s and Cs-s are not present in the PDOS while the states O-p, I-p and Cs-p dominate the top and the bottom of the VB. Moreover, we find out the overlapping of the states O-p and I-p in the VB top indicating the probable covalent character of the I-O bond but we observe a weak shift between O-p and Cs-p states positions with an narrow overlap indicative of a possible mixed "ionic-less accentuated covalent" Cs-O bond. In the conduction band (CB), there is some sharing of the Cs-d and the Cs-f states.

II.5.3. Charge densities

The electronic charge density shows us the nature of the bonds in compounds, whether they are ionic, covalent or even mixed in nature.

The calculation of the charge densities leads into the results interpreted in figure II.5. Each projection translates the contours of the charge density on a plane containing the four atoms Cs, I, and O.

There is clear spherical symmetries of charge densities around Cs atoms with a very slight deviations toward O atoms indication the predominately ionic Cs-O bond character. The deformed contours around I and O atoms (with both systems) illustrate the covalent character of I-O bonds which is in agreement with DOS results.

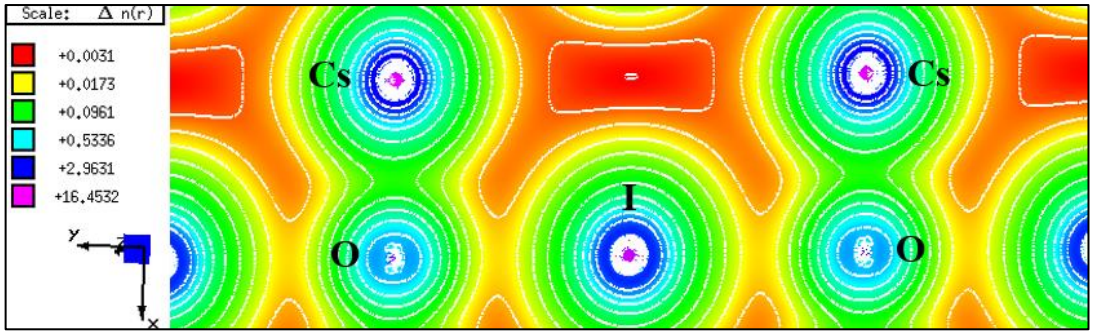


Figure II.5: charge density calculated for C-$CsIO_3$.

II.5.4. Liner optical properties

II.5.4.1. Dielectric function

The dielectric constant ε(ω) is the keystone for the exploitation and interpretation of the linear optical properties of materials. It is a complex function with a real part ε1(ω) and an imaginary part $\varepsilon_2(\omega)$.

The imaginary part of the dielectric function is calculated from the probabilities of electronic transitions between valence band and conduction band. Its formula is given by the following equation [11]:

$$\varepsilon_2(\omega)=(Ve^2/2\hbar\pi m^2\omega^2)\int d_3k\sum_{n,\,n'}|\langle \mathbf{k}n|\mathbf{p}|\mathbf{k}n'\rangle|^2 \times f(\mathbf{k}n)(1-f(\mathbf{k}n'))\delta(E_{\mathbf{k}n}-E_{\mathbf{k}n'}-\hbar\omega) \quad \ldots\ldots\ldots \text{II.1}$$

Where:

- V: cell volume.
- e: electron charge.
- m: electron mass.
- $\hbar\omega$: energy of the incident photon.
- $f(\mathbf{k}n)$: Fermi-Dirac distribution.
- p: angular momentum operator.
- $\mathbf{k}n$: wave function.

For the real part, the calculation is done using the following relation [12-14]:

$$\varepsilon_1(\omega)=1+(2/\pi)\int_0^{\infty}\{[\varepsilon_2(\omega).\omega'.d\omega']/[\omega'^2-\omega^2]\} \quad \ldots\ldots\ldots\ldots\ldots\ldots \text{II.2}$$

The calculations carried out on the dielectric functions (real parts ε1(ω) and imaginary parts ε2(ω)) led to the results illustrated in figure II.6.

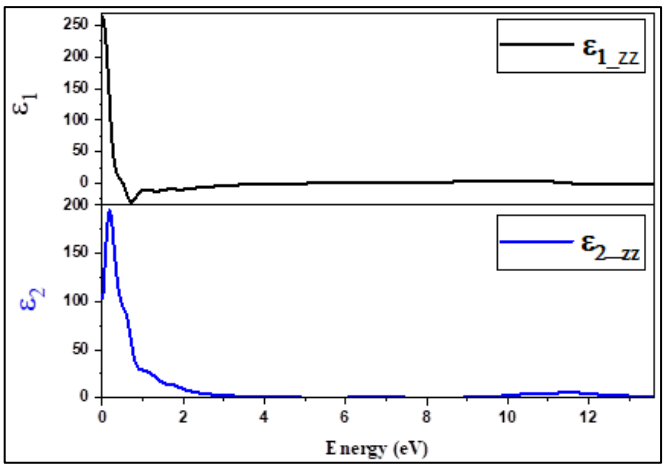


Figure II.6: Calculated imaginary ε2(ω) and real ε1(ω) parts of the dielectric function for C-$CsIO_3$ with TB-mBJ.

The first peak around 0.5 eV corresponds to transitions from O-p (VB) toward I-p (CB). Transitions of states I-5p (VB) toward O2p (CB) states also contribute in that region.

In the middle about 10-12 eV the narrow peak is mainly due to I5s (VB) and Cs-5p (VB) into O-2p and I-5p (BC). At about 15 eV, we make out transitions of states I-5s (VB) toward O-2p (CB) and of states O-2s (VB) toward I-5p (CB).

II.5.4.2. Static refraction indices

The static refractive indices are calculated from the real part of the dielectric function at $\varepsilon_1(0)$, this is its most important quantity. Table II.7 presents the obtained values.

Tableau II.7: Static refractive index calculated for C-$CsIO_3$.

C-$CsIO_3$	$n_x=n_y=n_z$
FP-LAPW	0.2631

II.5.4.3. Other linear optical properties

All other properties can be calculated from both the real and imaginary parts of the dielectric function:

- Absorption **I(ω)**: to estimate the optical gap.
- Reflectivity **R(ω).**
- Energy loss **L(ω)**: describes the energy of an accelerated electron passing through the crystal.
- Refractive index **n(ω).**

The equations II.4 to II.7 below allow the calculation of these properties.

$$I(\omega) = \sqrt{2}\omega.[\sqrt{\varepsilon_1^2(\omega)+\varepsilon_2^2(\omega)} - \varepsilon_1(\omega)^{1/2} \quad \text{..... (II.3)}$$

$$R(\omega) = [(\sqrt{\varepsilon(\omega)} - 1)/(\sqrt{\varepsilon(\omega)} + 1)]^2 \quad \text{..... (II.4)}$$

$$L(\omega) = \varepsilon_2(\omega)/(\varepsilon_1^2(\omega)+\varepsilon_2^2(\omega)) \quad \text{..... (II.5)}$$

$$n(\omega) = 1/\sqrt{2}.[\sqrt{\varepsilon_1^2(\omega)+\varepsilon_2^2(\omega)}+ \varepsilon_1(\omega)]^{1/2} \quad \text{..... (II.6)}$$

The calculation results obtained for these four parameters are illustrated in figures II.7.

In the energy loss **L(ω)** diagram, the most important pic corresponds to the plasma frequency **ωp** where we notice a sharp reduction in reflectivity **R(ω)**. Values of energies corresponding to those characteristic pics are grouped in table II.8.

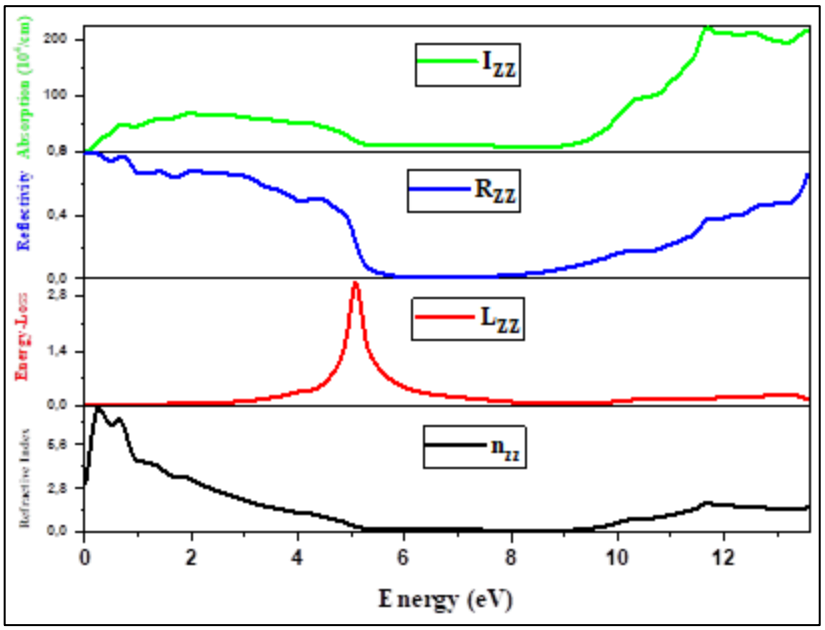


Figure II.7 Calculated optical properties for C-$CsIO_3$ as function of the incident photon energy (eV): absorption coefficient **I** (10^4/cm), reflectivity **R**, energy loss **L**, and refraction index **n**.

Tableau II.8: Energy loss L(ω) for C-$CsIO_3$ (10^4/cm).

C-$CsIO_3$	**Energy loss L(ω) at ωp (10^4/cm)**
	$L(\omega\rho)_{xx}=L(\omega\rho)_{yy}=L(\omega\rho)_{zz}$ (eV)
FP-LAPW	3.139

From the absorption spectra I(ω) we can derive the values of the optical gaps of our material. The values for C-$CsIO_3$ are represented in table II.9.

Tableau II.9: Optical gap values (energy at I_0) for C-$CsIO_3$.

C-$CsIO_3$	**Energy at I_0 ≡ optical gap (eV)**
	$E[I(0)_{xx}]=E[I(0)_{yy}]=E[I(0)_{zz}]$)
FP-LAPW	0.431

Table II.10: Values of the birefringence (Δn) for the compound C-$CsIO_3$.

C-$CsIO_3$	**Birefringence (Δn)**			
	At the static limit		**Maximum value (energy in eV)**	
	xx-yy	**yy-zz**	**xx-yy**	**yy-zz**
WC-GGA	0	0	0	0

II.6. Conclusion

From the reported results, we can conclude that our material is a semiconductor of choice with a more or less wide transparency window. Also, from the calculated properties, we

found that TB-mBJ considerably improves the estimation of the electronic properties and especially that of the bandgap.

On the other hand, the choice of approximation turns out to be important because the results of the calculated properties change from one approximation to another.

References

[1]: P. Blaha; K. Schwarz; G.K.H. Madsen; D. Kvasnicka; J. Luitz; R. Laskowski; F. Tran; L.D. Marks, "WIEN2K An augmented plane wave plus local orbitals program for calculating crystal properties", Vienna University of Technology, Austria, (2018).

[2]: W. H. Zachariasen, *Skrifter utgitt av det Norse Videnskaps-Akademi I Oslo 1: Matematisk-Naturvidenskapelig Klasse* 1928 (1928) 1.

[3]: J. C. Slater. Phys. Rev. 51, (1937) 846.

[4]: K. P. Perdew, K. Burke, M. Ernzerhof, Phys. Rev. Lett. 77(18) (1996) 3865.

[5]: K. Schwarz, P. Blaha, G. K. H. Madsen, Computer Physics Communications 147 (2002) 71.

[6]: S. Baroni, S. de Gironcoli, A. Dal Corso, and P. Giannozzi. Rev. Mod. Phys. 73, (2001) 515.

[7]: H. B. Schlegel. J. Comp. Chem. 3. 214 (1982).

[8]: F. Tran, P. Blaha, Phys. Rev. Lett. 102 (2009) 226401.

[9]: K. Momma, F. Izumi, J. Appl. Cryst. 44 (2011) 1272: VESTA (Visualization for electronic and structural analysis) Ver. 3.4.2. (2017).

[10]: B. Lagoun, B. Bentria, I. K. Lefkaier, Physica B 433 (2014) 117.

[11]: S. Saha, T. P. Sinha, Physical Review B 62(13) (2000) 8828.

[12]: H. A. Kramers, Nature 113(2845) (1924) 673.

[13]: H. A. Kramers, Nature 114(2845) (1924) 310.

[14]: R. DE L. Kronig, J. Opt. Soc. America 12(6) (1926) 547.

General conclusion

The current research represents an exhaustive theoretical analysis of structural, electronic, and optical properties of the cubic phase of cesium iodate (C-$CsIO_3$). In the present work, first-principles calculations based on Density Functional Theory (DFT) are performed using WIEN2K code.

The first part of this thesis is dedicated to a systematic literature survey where the basic fundamentals of nonlinear optical (NLO) materials are discussed, the approaches for designing non-centrosymmetric (NCS) structures are described, and the importance of stereochemically active lone pairs in causing distortion effects is explained. It is stated that the most promising class of NLO materials among all known to date is the iodate group. The latter possesses an interesting structure, namely a distorted trigonal pyramid with a large local dipole moment of the central I^{5+} cation. Moreover, the computational techniques used in the existing studies such as FP-LAPW, GGA approach, and TB-mBJ (modified Becke-Johnson potential) are discussed in detail.

In the second chapter, we used ab initio calculations for studying the cubic primitive crystal structure of C-$CsIO_3$ (Pm-3m, N° 221) based on the WC-GGA exchange-correlation functional complemented with the TB-mBJ potential. The lattice optimization was done with the help of the BFGS algorithm and led to quite realistic values of the structural parameters with the error of around 4.31% for the lattice constant and 12.44% for the volume of the unit cell; values typical for the underestimation of the equilibrium volumes in structures containing elements with high atomic mass using GGA-type functionals.

The calculation of the electronic structure in the framework of TB-mBJ potential showed that C-$CsIO_3$ in its cubic modification is characterized by a metallic type of the band structure (Eg=0 eV). In turn, the density of states analysis helped to determine which atomic orbitals from Cs, I, and O atoms responsible for valence and conduction bands. More specifically, the analysis showed that the valence band in this case mainly contains O-2p states, whereas the conduction band mainly consists of I-5p and Cs states.

Linear optical properties were determined using the complex dielectric function $\varepsilon(\omega)$ which was calculated using TB-mBJ technique. Imaginary part of the dielectric function $\varepsilon_2(\omega)$ was calculated based on interband electronic transitions, whereas the real part $\varepsilon_1(\omega)$ was calculated by applying the Kramers-Kronig transformation. Using these quantities,

we determined the following properties: absorption coefficient I(ω), reflectivity R(ω), energy loss function L(ω), and refractive index n(ω) in all crystallographic directions. In addition, the values of static refractive index and birefringence Δn were determined, which confirmed the optical isotropy of cubic structure at the static limit.

In summary, this study shows that the combination of the TB-mBJ potential with the structural refinement using the WC-GGA exchange-correlation functional in the FP-LAPW approach is an efficient method to calculate the physical characteristics of $CsIO_3$. Results obtained in this study can help gain insight into the electronic and optical behavior of this material when it crystallizes in its high-symmetry cubic form, allowing us to provide a theoretical foundation for future research on different aspects, such as the study of lower-symmetry phases, phase transitions induced by heating, and the study of SHG associated with $CsIO_3$ polymorphs.

In terms of future perspectives, one would find it very interesting to apply this computational methodology to the investigation of other lower-symmetry forms of $CsIO_3$, such as monoclinic and rhombohedral phases, which are non-centrosymmetric and able to perform SHG. In addition, the utilization of more accurate exchange-correlation functionals and the consideration of spin-orbit coupling due to the presence of elements with heavy masses would allow improving the quality of calculated results. Finally, the synthesis of the material and experimental study of its optical behavior would be highly appreciated.

عنوان المذكرة: دراسة نظرية للخصائص البنيوية والإلكترونية والبصرية ليودات السيزيوم المكعب $C\text{-}CsIO_3$

اللقب: هازل، بن الطيرش **الإسم**: محمد طه، عبد الحميد **المؤطرة**: د. بلحاج صوراية

ملخص:

تتناول هذه المذكرة دراسة من المبادئ الأولى لمركب يودات السيزيوم المكعب $C\text{-}CsIO_3$ باستعمال نظرية دالة الكثافة (DFT). تم دراسة الخصائص البنيوية والإلكترونية والبصرية الخطية باستخدام برنامج WIEN2k وطريقة FP-LAPW مع جهد TB-mBJ.

أظهرت النتائج معلومات حول البنية الحزمية وكثافة الحالات والدالة العازلية ومعامل الانكسار والسلوك البصري للمادة. كما بينت الدراسة أن مركب $CsIO_3$ يمتلك خصائص مناسبة للتطبيقات البصرية والإلكترونيات الضوئية.

الكلمات المفتاحية: $C\text{-}CsIO_3$، DFT، WIEN2k، الخصائص البصرية.

Memory title: **Theoretical Investigation of the Structural, Electronic, and Optical Properties of Cubic Cesium Iodate $C\text{-}CsIO_3$**

Name: **HAZEL, BENTIRECHE** **First name:** **Mohamed Taha, Abdelhamid** **Directed by:** **Dr. S. BELHADJ**

Abstract:

This thesis presents a first-principles study of cubic cesium iodate $C\text{-}CsIO_3$ using density functional theory (DFT). Structural, electronic, and linear optical properties were investigated using the WIEN2k code within the FP-LAPW method and the TB-mBJ potential.

The obtained results provide information about the band structure, density of states, dielectric function, refractive index, and optical behavior of the material. The study shows that $C\text{-}CsIO_3$ possesses interesting properties for optical and optoelectronic applications.

Keywords: $C\text{-}CsIO_3$, DFT, WIEN2k, Optical Properties.

Titre du mémoire: **Étude théorique des propriétés structurales, électroniques et optiques de l'iodate de césium cubique $C\text{-}CsIO_3$**

Nom: **HAZEL, BENTAIRECHE** **Prénom : Mohamed Taha, Abdelhamid** **Encadreur : Dr. S. BELHADJ**

Résumé :

Ce mémoire présente une étude ab initio de l'iodate de césium cubique $C\text{-}CsIO_3$ à l'aide de la théorie de la fonctionnelle de la densité (DFT). Les propriétés structurales, électroniques et optiques linéaires ont été étudiées à l'aide du code WIEN2k dans le cadre de la méthode FP-LAPW et du potentiel TB-mBJ.

Les résultats obtenus donnent des informations sur la structure de bandes, la densité d'états, la fonction diélectrique, l'indice de réfraction et le comportement optique du matériau. Cette étude montre que $C\text{-}CsIO_3$ possède des propriétés intéressantes pour les applications optiques et optoélectroniques.

Mots-clés : $C\text{-}CsIO_3$, DFT, WIEN2k, Propriétés optiques.